

Charge-induced conformational changes of dendrimers

Ronald Blaak, Swen Lehmann,* and Christos N. Likos

Institut für Theoretische Physik II: Weiche Materie,

Heinrich-Heine-Universität Düsseldorf, Universitätsstraße 1, D-40225 Düsseldorf, Germany

(Dated: April 9, 2008, submitted to *Macromolecules*)

We study the effect of chargeable monomers on the conformation of dendrimers of low generation by computer simulations, employing bare Coulomb interactions. The presence of the latter leads to an increase in size of the dendrimer due to a combined effect of electrostatic repulsion and the presence of counterions within the dendrimer, and also enhances a shell-like structure for the monomers of different generations. In the resulting structures the bond-length between monomers, especially near the center, will increase to facilitate a more effective usage of space in the outer-regions of the dendrimer.

Keywords: Dendrimers, Molecular Dynamics Simulations, Polyelectrolytes, Scattering

I. INTRODUCTION

Dendrimers have been the subject of intensive investigations ever since their synthesis¹ in the late 1970s. They are characterized by a high degree of monodispersity and a well-defined, highly branched internal structure; efficient dendrimer assembly has been boosted by recent progress in synthetic techniques.² A great deal of research activity has focused on the issue of whether they possess an open, *dense-shell* or a collapsed, *dense-core* configuration, the motivation arising by the potential to employ them as hollow, carrier-type molecules in the former case. For neutral dendrimers, a large number of simulation studies,³ careful self-consistent field calculations⁴ and not least scattering experiments^{5,6} have revealed that the dense-shell conformation is *not* the real one. Due to back-folding of the end-groups, caused by entropic considerations, a dense-core calculation results instead, leading even to compact, hard-sphere-like conformations at high generation numbers.^{7,8} From the point of view of applications, this may sound like a disappointing result, as one would like to have dense-shell molecules. However, seen from the angle of fundamental research, the growing compactness of dendrimers with increasing generation number is very welcome, since it allows to use them as model colloidal/nano particles with tunable stiffness,^{9,10} bridging the gap between flexible polymers and rigid spheres.

The issue of dendrimer conformations is less clear when *charged* or *polyelectrolyte* dendrimers are considered. Charge on the building blocks of, e.g., poly(amidoamine) (PAMAM) dendrimers can be manipulated by changing the pH of the solution¹¹ and their conformations can be further influenced by added salt. The expectation that charged dendrimers may achieve stretching is based on experience with other branched polyelectrolytes (PE), such as PE-stars, for instance.¹² However, the SANS-study of Nisato *et al.*¹¹ has led to a negative result: the size of dendrimers is insensitive to pH changes and thus to charge. This experimental fact is at odds with the earlier work by Welch and Muthukumar,¹³ who predicted, by means of simulation and theory, an ‘opening up’ of PE

dendrimers upon increase of the number of charged units; similar conclusions were reached in the Brownian Dynamics simulations of Lyulin *et al.*¹⁴ However, both simulational works quoted above employed a Debye-Hückel (screened Coulomb) interaction potential acting between charged units, treating thereby the counterions as a continuum. Giupponi *et al.*, on the other hand, pointed out that a more realistic treatment of the molecules should employ the bare Coulomb interactions among all involved species (monomers and counterions), which is the method they employed in their own, recent simulations.¹⁵ Interestingly enough, they found that the dendrimer size is indeed very weakly dependent on charge, due to local charge neutrality, a condition that is masked when one employs the Debye-Hückel approximation.

Though the work of Giupponi *et al.*¹⁵ has illuminated a number of issues pertaining to monovalently charged monomer units accompanied by monovalent counterions, the question of the influence of valency on dendrimer conformations has not been studied so far. The purpose of this work is to examine precisely this issue, which appears relevant on the grounds that counterion valency is known to bring about drastic changes in, e.g., the size of spherical PE brushes.¹⁶ We focus thereby on dendrimers of the fourth generation ($G = 4$) and examine separately the conformations of neutral dendrimers, as a reference point, as well as the combinations $(Z_m, Z_c) = (1, 1), (1, 2), (2, 1)$ and $(2, 2)$, where Z_m stands for the valency of the monomers and Z_c for the valency of the counterions. We find that the case of divalent monomers and monovalent counterions brings about a substantial change of the dendrimer size, accompanied by a strong stretching of the chemical bonds, whereas the same phenomena are less pronounced for the other two cases. After describing our simulation model in Sec. II, we present and discuss the results in Sec. III, whereas in Sec. IV we draw our conclusions.

II. THE SIMULATION MODEL

The dendrimers we use within our simulations are built from a central pair of joined monomers, the so-called generation 0. A successive generation $g + 1$ of dendrimer is formed by connecting two additional monomers, the functionality of the dendrimer is therefore three, to each outer monomer of the dendrimer of generation g . In doing so, the number of monomers $n(g)$ of a given generation g in a dendrimer follows a simple power law, i.e. $n(g) = 2^{g+1}$.

There are in general three types of interactions between monomers. The first type of interaction prevents the collapse of monomers onto each other and is a short-range repulsive interaction given by a simple, shifted and purely repulsive Lennard-Jones potential

$$V_{LJ} = \begin{cases} 4\epsilon \left[\left(\frac{\sigma}{r} \right)^{12} - \left(\frac{\sigma}{r} \right)^6 + \frac{1}{4} \right] & r \leq r_c \\ 0 & r > r_c \end{cases} \quad (1)$$

where σ and ϵ are the unity of length and energy respectively, and $r_c = 2^{1/6}\sigma$ is the range of the interaction.

The second type of interaction is of an attractive nature and describes the bonds between joined monomers in order to prevent the molecule from flying apart. This interaction is described by a FENE potential¹⁷

$$V_{FENE} = \begin{cases} -15\epsilon \left(\frac{R_0}{\sigma} \right)^2 \ln \left[1 - \left(\frac{r}{R_0} \right)^2 \right] & r \leq R_0 \\ 0 & r > R_0 \end{cases} \quad (2)$$

where $R_0 = 1.5\sigma$ is the maximum allowed distance between two connected monomers.

The last type of interaction to be included in the model is the Coulomb potential between charged monomers

$$V_{Coulomb} = k_B T \lambda_B \frac{Z_i Z_j}{r_{ij}} \quad (3)$$

with Z_i and Z_j the charge numbers, k_B the Boltzmann constant, T the temperature, and λ_B the Bjerrum length given by

$$\lambda_B = \frac{e^2}{\epsilon_r k_B T} \quad (4)$$

We have performed molecular dynamics simulations at constant density and temperature using the Nosé-Hoover thermostat^{18,19} on dendrimers of generation 4, i.e., a dendrimer formed by 62 identical monomers, where the monomers with charge number Z_m are either neutral, monovalent, or divalent. In order to guarantee charge neutrality the charged dendrimers need to be balanced, for which we in either case used both monovalent and divalent counterions (charge number Z_c). Apart from the Coulomb interaction between monomers and counterions, as well as between the counterions themselves, we use for simplicity the same short range repulsion (1) as is used for the monomers.

Simulation parameters are chosen such that our unit of length $\sigma = 2.84\text{\AA}$ and we fixed the temperature to

$T = 1.2\epsilon/k_B$. Using an implicit solvent that mimics the behavior of water, i.e., a temperature of 300K and a relative permittivity $\epsilon_r = 80$ we arrive at $\lambda_B/\sigma = 3$. Periodic boundary conditions have been applied in combination with the Ewald summation method to include the long-range electrostatic interactions. The volume of the simulation box was chosen such that effectively the dendrimers can be considered to be independent, indicated by the independence of the results on larger volume sizes. The initial configurations were equilibrated over times long enough for the counterions to diffuse in to the core of the dendrimer, and to reach a steady state for a in- and out-flux. The simulation time is chosen long enough for the individual counter-ions to explore the full dendrimer, i.e., inner and outer ranges.

III. RESULTS

In order to characterize the size of the dendrimer, the radius of gyration R_g is measured, which is defined by

$$R_g^2 = \left\langle \frac{1}{N} \sum_{i=1}^N (\vec{r}_i - \vec{r}_{CM})^2 \right\rangle, \quad (5)$$

where the summation runs over the N positions \vec{r}_i of the monomers of the dendrimer and \vec{r}_{CM} is the center of mass of the dendrimer.

The resulting values for the neutral and charged dendrimers are listed in Table I. The first observation we can make, is that by charging the dendrimer the radius of gyration increases. This is actually not so surprising, because the monomers will repel each other due to their charges. What is more interesting is the fact that the behavior on charging is not monotonic, i.e., the radius of gyration of the divalently charged monomers and counterions is smaller with respect to that of the monovalent case. This suggests that the swelling of the dendrimer due to the increasing charge is counteracted by the transport of counterions into the deeper regions of the dendrimer, which results in screening effects and reduces the swelling.^{20,21,22}

$Z_m - Z_c$	R_g^2/σ^2	R_g/σ
neutral	6.31 ± 0.02	2.51 ± 0.01
1-1	8.20 ± 0.02	2.86 ± 0.01
1-2	7.12 ± 0.02	2.67 ± 0.01
2-1	9.27 ± 0.02	3.04 ± 0.01
2-2	7.49 ± 0.02	2.74 ± 0.01

TABLE I: The radius of gyration for the neutral dendrimer and the dendrimers with charged monomers and counterions, with charge numbers Z_m and Z_c respectively.

It also appears that divalent counterions reduce the size of the dendrimer with respect to that of monovalent counterions. Not only do they result in a better screening of the monomers, but also less of them are required

which also leads to less steric hindrance. Using a similar argument, the monovalent monomers reduce the size of the dendrimer with respect to that of divalent monomers, because in the latter case more counterions are required within the dendrimer, preventing its shrinking. Note that for a neutral dendrimer there is no counterpart for the counterions present within the dendrimer, hence it is only the short-range repulsion between the monomers that prevents the dendrimer from collapsing.

The radius of gyration is also experimentally observable from the small wave-vector limit of the form factor $F(\vec{q})$ defined by

$$F(\vec{q}) = 1 + \frac{1}{N} \left\langle \sum_{i \neq j} \exp(-i\vec{q} \cdot \vec{r}_{ij}) \right\rangle. \quad (6)$$

By expanding in small wave-vectors q and averaging over the directions it is easy to show that this results in

$$F(q) = N \left[1 - \frac{(qR_g)^2}{3} \right]. \quad (7)$$

In the present case this expansion is valid up to $q\sigma \approx 0.2$ as can be seen in Fig. 1 where we compare the measured form factor, Eq. (6), from the simulation (sim), with the small wave-vector limit, Eq. (7), denoted (th).

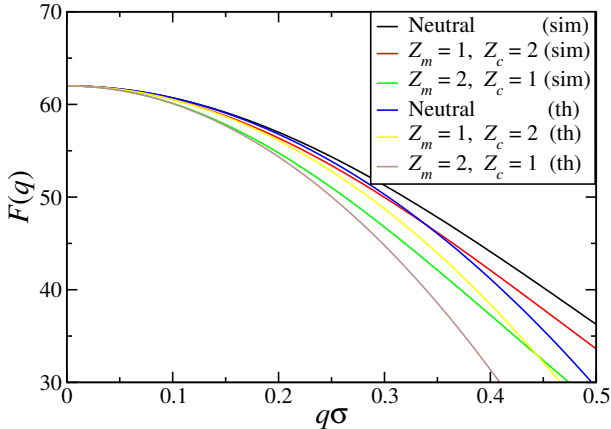


FIG. 1: Comparison of the measured form factor, Eq. (6) from the simulation (sim), with the small wave-vector limit, Eq. (7), denoted (th).

In Fig. 2 the radial density profiles of the monomers and counterions are shown, both measured with respect to the center of mass of the dendrimer. Note that at small distances from the center of mass the noisy behavior is purely due to a poor statistical sampling caused by the lack of particles in that region.

It is immediately clear that the presence of charge on the monomers results in a much more structured density profile, in which the monomers are mostly found in a shell-like structure. The mutual repulsion of the monomers due to their charge not only leads to a larger size of the dendrimer but it enables the counterions to

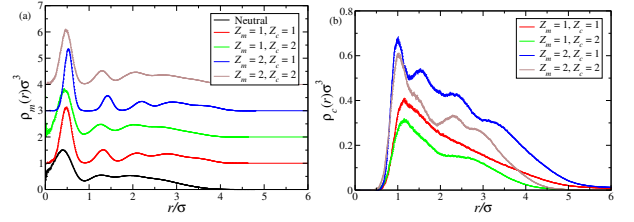


FIG. 2: Radial density profiles for the monomers (a) and counterions (b), measured with respect to the center-of-mass of the dendrimer. The curves in the left-hand figure have been shifted to facilitate a comparison.

diffuse into the dendrimer as well; this can be seen from their density profiles. Their distribution, however, shows less structure and has a wider range. The latter can also easily be understood, since the presence of counterions within the dendrimer will also lead to steric hindrance and there is an obvious entropic gain in surrounding the dendrimer and move in the region lying outside its extent.

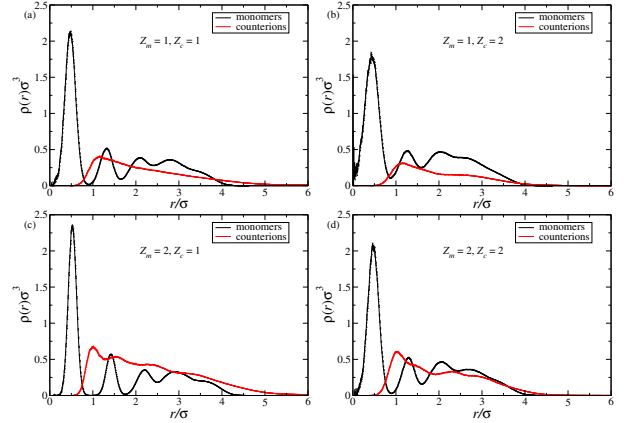


FIG. 3: Radial density profiles of the monomers and counterions for the monovalently [(a),(b)] and divalently [(c),(d)] charged monomers, and monovalently [(a),(c)] and divalently [(b),(d)] counterions.

To clarify the ordering in the charged dendrimer cases, the same data are shown in Fig. 3 where the radial density profiles of the monomers and counterions are directly compared. Although the highest density for the counterions is reached roughly in between the first and second peak of the monomer distributions (except for the case $Z_m = 1$ and $Z_c = 2$), there is no layered structure present for the counterions. This is also confirmed by the absence of plateaus in the cumulative counterion density profile (not shown).

The absence of charges on the monomers in the neutral dendrimer does not only affect its size, i.e., it is more compact, but it also modifies its internal structure as is illustrated in Fig. 4, where the density profiles for the different generations are plotted versus the distance to the center of mass. This reveals that the density of generation 4 monomers at smaller distances is larger than

that of those from generation 3. In other words, the dendrimer starts to fold in to itself. Whereas the repulsive Coulomb interactions between charged monomers tend to stretch the dendrimer causing a loss in entropy, the neutral monomers just feel the short-range Lennard-Jones repulsion and can exploit the open space in the core of the dendrimeric structure. A not unimportant other reason is the absence of the equivalent of counterions within the dendrimer. This effect is only weakly visible in the cases of the divalently charged counterions, but it is to be expected that it will be more pronounced for increasing value of the generation of the dendrimer.

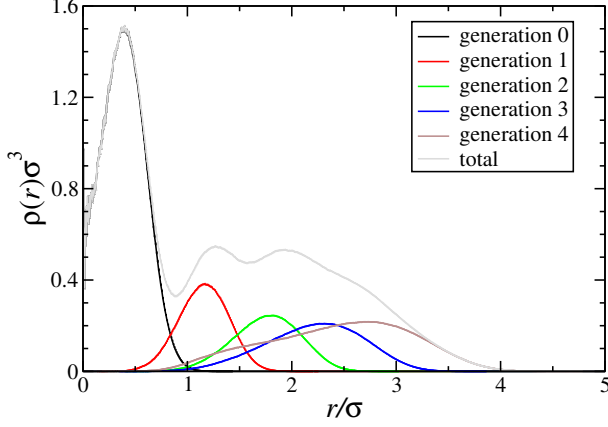


FIG. 4: Radial density profiles of the monomers in the neutral dendrimer decomposed in the contributions stemming from each generation.

A more detailed description of the internal structure of the dendrimer can be obtained by analyzing the the bond-lengths b , shown in Figs. 5 and 6. The bond-length probability distributions, $P(b)$, are decomposed per generation, whereby a bond of generation n is formed by a monomer of generation g with its parent of generation $g - 1$ (with the exception of generation 0). For the neutral dendrimer only a small shift in the distribution of lengths is found towards shorter bond-lengths for higher generations, i.e., bonds near the center of the dendrimer tend to be more stretched than those near the border. This implies that there is a collective behavior in which the mutual repulsion of monomers in higher generations that prefers to expand the dendrimer, forcing the fewer central bonds to stretch.

Fig. 6 shows the same distributions but now for the charged dendrimer cases. The first thing one can observe is that the bond-lengths in the charged cases are more stretched. This is not so surprising, since the bond-length is directly affected by the mutual charge repulsion of the monomers and even more so for the divalent monomers. Also the tendency for the central bonds to be more stretched than those in the outer regions is apparent. The most interesting case, however, is that of the divalent monomers and monovalent counterions, in which case the stretching of the bond-lengths shifts significantly with the generation. In Fig. 7 this is illustrated

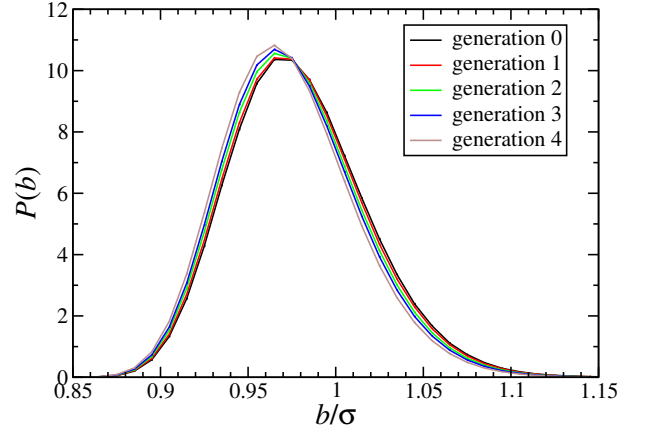


FIG. 5: Probability distribution of bond-lengths for each generation for the neutral dendrimer.

even more clearly by comparing the bonds of generation 0 and 4 for the various models. This suggests that the abundance of monovalent counterions required for an effective screening of the divalent monomer bonds can not be packed within the core of the dendrimer.

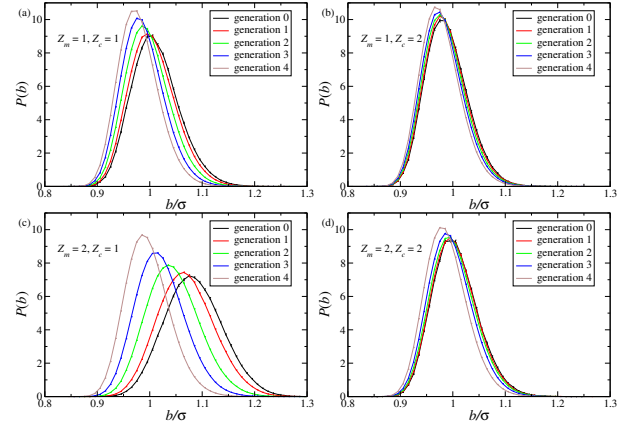


FIG. 6: Probability distribution of bond-lengths for each generation for the monovalently [(a),(b)] and divalently [(c),(d)] charged monomers, and monovalently [(a),(c)] and divalently [(b),(d)] charged counterions.

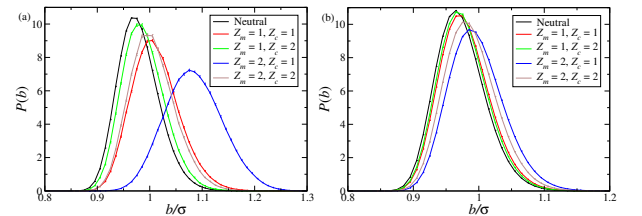


FIG. 7: Probability distribution of bond-lengths of generation 0 (a) and generation 4 (b) for the different cases monomers and counterions.

In the final method we used to examine the internal structure of the dendrimer, we consider the angles be-

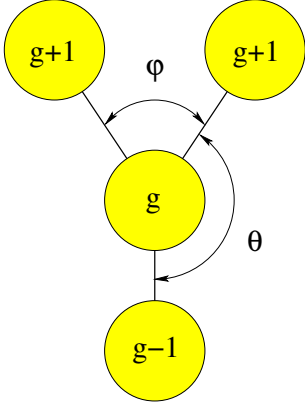


FIG. 8: Schematic representation of the local structure of a monomer inside a dendrimer indicating the different θ and ϕ angles mentioned in the text.

tween bonds in the dendrimer. The angle ϕ as illustrated in Fig. 8 is the angle between the bonds of a monomer of generation g and the two monomers bounded to it of generation $g+1$ (a bond generation $g+1$). The angle θ is the angle between a bond of generation g and a bond of generation $g+1$.

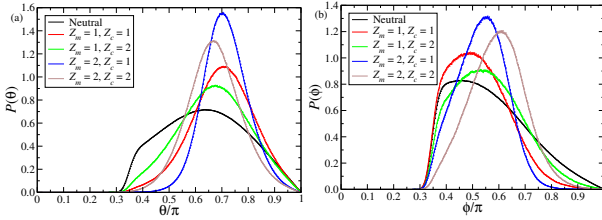


FIG. 9: Probability distribution of the angles θ [(a)] and ϕ [(b)] for the different dendrimer cases averaged over all nodes in the dendrimer.

The results of the angle analysis are shown in Fig. 9, where we have averaged over all 30 nodes in the dendrimer. In the case of the neutral dendrimer the probability distributions are broader than in the case of the charged dendrimers. This is partially due to the fact that there is no penalty for smaller angles, whereas in the charged dendrimer cases the angles will be more focused in the equal angles area due to the Coulomb repulsion.

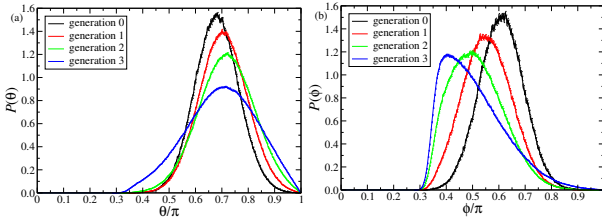


FIG. 10: Probability of the angle distributions of a dendrimer with monovalent monomers and counterions. (a): angle θ ; (b): angle ϕ .

Also these angle distributions will, just like in the case of the bond-lengths, depend on the position of the monomer within the dendrimer, i.e. its generation, as can be seen in Fig. 10 in the case of monovalent monomers and dendrimers. For nodes near the core the ϕ angles are more or less centered about 120° , but for nodes near the boundary of the dendrimer the peaks shifts to smaller angles. This is specially clear for the angle ϕ for the outer most nodes lies between 70° and 80° for the various cases presented here. At the same time the θ angles show a similar behavior, except that they become larger, albeit that the shift is not as significant as is the case for ϕ .

This is not the only information that can be extracted from the angles θ and ϕ . In general the three bonds at a given node will not lie within a single plane, but span a space angle, also called spherical excess,²³ ε , which ranges from zero to 2π . Both extremes can only be obtained in the limiting case of three bonds lying within the same plane. The fact that for such a planar configuration the spherical excess can take two values can be understood by realizing that two cases need to be distinguished. If the sum of the three angles between the pairs of bonds $\theta_1 + \theta_2 + \phi = 2\pi$, the space angle reaches its maximum 2π and spans a half sphere. In the other case the largest of the three bond angles equals the sum of the smaller ones, e.g. $\theta_1 + \theta_2 = \phi$ and the spherical excess reaches its minimum 0. In other words, when the three bonds completely open up and stretch away from one another, one has the maximum value, $\varepsilon = 2\pi$; on the other hand, when there is complete backfolding of the two bonds connecting the g -monomer with the two $g+1$ -monomers towards the bond between the g -monomer and the $g-1$ -monomer in Fig. 8, then $\varepsilon = 0$. In this fashion, the probability distribution $P(\varepsilon)$ of the spherical excess offers valuable information on the presence of back-folding within the dendrimer. A distribution with strongly suppressed values around $\varepsilon = 0$ and high values around $\varepsilon = 2\pi$ implies a stretched dendrimer with planar three-bond junctions at the branching points. Relatively flat distributions with non-negligible values around $\varepsilon = 0$ point rather to strongly back-folded dendrimers, akin to neutral ones.

The probability distribution of the spherical excess for the neutral dendrimer and for the case of a charged dendrimer with both monomers and counterions monovalently charged, is shown in Fig. 11. It reveals that the spherical excess decreases for nodes that lie further away from the core of the dendrimer. The preference for spherical excess to be large near the center of the dendrimer can be understood by realizing that such behavior will maximize stretching in the dendrimer and enable to exploit the so available space for the more distant monomers more effectively. The decrease of the spherical excess is particularly striking in the case of the neutral dendrimer and is a necessary consequence from our earlier observation that the monomers from the last generation can fold back into the dendrimer.⁷ As can be seen in Fig. 11(b), however, and in conjunction with Fig. 11(a),

the $Z_m = Z_c = 1$ -dendrimer shows a considerably higher degree of stretching than the neutral one; its distribution of the spherical excess is shifted towards higher values and only at the third generation do we observe a nonvanishing contribution around $\varepsilon = 0$.

Fig. 12 shows the spherical excess of the nodes of generation 0 and 3 for the various models discussed. In full agreement with all our previous measures, we find that charged dendrimers carrying divalent monomers and monovalent counterions show the most dramatic degree of stretching, all the way from the inner to the outermost generations. Physically, this is caused by the strong attraction between the monomers and the counterions. In this case, there are twice as many counterions as in the cases $Z_m = Z_c = 1$ and $Z_m = Z_c = 2$ that have to be accommodated in the inner region of the dendrimer, giving rise to stretching to create space. Two counterions per monomer are required to achieve local charge neutrality,¹⁵ rendering the composite, monomer-counterion groups too big to allow for the backfolding seen for neutral dendrimers.

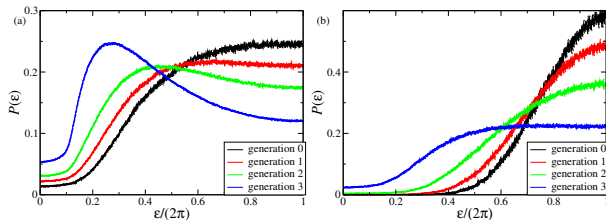


FIG. 11: Spherical excess for the neutral dendrimer [(a)] and monovalently charged monomers and counterions [(b)].

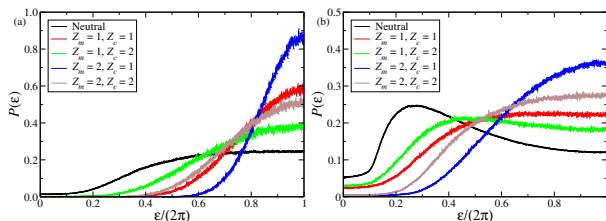


FIG. 12: Spherical excess of generation 0 [(a)] and generation 3 [(b)] nodes for the different cases monomers and counterions.

IV. DISCUSSION

We have presented simulation data of simple, fourth generation dendrimers and investigated the effect that

chargeable monomers will have on their size and internal structure. In particular, we have allowed for the possibility of divalent monomer units and/or counterions and monitored the conformational changes induced by the various scenarios. For the simplest case, $Z_m = Z_c = 1$, our findings are in full agreement with the recent ones of Guipponi *et al.*,¹⁵ in the sense that no dramatic changes in the dendrimer conformation and size have been detected. This is also in agreement with the experimental results of Nisato *et al.*¹¹ and at odds with the prediction of Welch and Muthukumar.¹³ At this point, it appears that the assumption of linear counterion screening, which has been employed in Ref. 13 in the form of a Debye-Hückel approximation, is not valid when strong counterion absorption and condensation effects are present. More so at the nanoscale-distances involved in the inner of a dendrimer.

At the same time, we could establish that a remarkable change of the size of the dendrimer, accompanied by a stiffening and stretching of its bonds, takes place when the former carries divalent chargeable groups, which release two monovalent counterions per site. Here, although the resulting configuration is not yet of the dense-shell type, the dendrimer size grows by almost 50% in comparison to a neutral dendrimer and strong correlations between the monomer- and counterion profiles appear. It is now reasonable to assume that, given a guest molecule that carries the same type of charge as the counterions and being small enough to ‘fit’ inside the stretched dendrimer, absorption will take place, as in this fashion a number of counterions will be released from the inner part of the dendrimer, resulting in a concomitant entropy gain.^{24,25,26,27,28,29} Another possibility is to endow the dendrimers with a spacer length $s > 1$, which allows for creation for more space in their interior but at the same time it also increases the possibilities to backfolding. Work along these lines is currently in progress.

Acknowledgments

This work has been supported by the Deutsche Forschungsgemeinschaft (DFG).

* Current address: Institut für Physikalische Chemie, RWTH Aachen, Landoltweg 2, D-52056 Aachen, Germany

¹ Buhleier, G. E.; Wehner, W.; Vögtle, F. *Synthesis*

(Stuttgart) **1978**, 2, 155.

² Antoni, P.; Nystrom, D.; Hawker, C. J.; Hult, A.; Malkoch, M. *Chem. Commun.* **2007**, 22, 2249.

- ³ See, e.g., Ballauff, M.; Likos, C. N. *Angew. Chem. Intl. Ed.* **2004**, *43*, 2998 and references therein.
- ⁴ Zook, T. C.; Pickett, G. *Phys. Rev. Lett.* **2003**, *90*, 015502.
- ⁵ Pötschke, D.; Ballauff, M.; Lindner, P.; Fischer, M.; Vögtle, F. *Macromolecules* **1999**, *32*, 4079.
- ⁶ Pötschke, D.; Ballauff, M.; Lindner, P.; Fischer, M.; Vögtle, F. *Macromol. Chem. Phys.* **2000**, *201*, 330.
- ⁷ Götze, I. O.; Likos C. N. *Macromolecules* **2003**, *36*, 8189.
- ⁸ Rathgeber, S.; Monkenbusch, M.; Kreitschmann, M.; Urban, V.; Brulet, A. *J. Chem. Phys.* **2002**, *117*, 4047.
- ⁹ Likos C. N.; Rosenfeldt S.; Dingenouts N.; Ballauff, M.; Lindner, P.; Werner, N.; Vögtle, F. *J. Chem. Phys.* **2002**, *117*, 1869.
- ¹⁰ Götze, I. O.; Harreis, H. M.; Likos, C. N. *J. Chem. Phys.* **2004**, *120*, 7761.
- ¹¹ Nisato, G.; Ivkov, R.; Amis, E. J. *Macromolecules* **2000**, *33*, 4172.
- ¹² Jusufi, A.; Likos, C. N.; Löwen, H. *Phys. Rev. Lett.* **2002**, *88*, 018301.
- ¹³ Welch, P.; Muthukumar, M. *Macromolecules* **2000**, *33*, 6159.
- ¹⁴ Lyulin, S. V.; Evers, L. J.; van der Schoot, P.; Darinskii, A. A.; Lyulin, A. V.; Michels, M. A. J. *Macromolecules* **2004**, *37*, 3049.
- ¹⁵ Guipponi, G.; Buzza, D. M. A.; Adolf, D. B. *Macromolecules* **2007**, *40*, 5959.
- ¹⁶ Mei, Y.; Lauterbach, K.; Hoffmann, M.; Borisov, O. V.; Ballauff, M.; Jusufi, A. *Phys. Rev. Lett.* **2006**, *97*, 158301.
- ¹⁷ Grest, G. S.; Kremer, K.; Witten T. A. *Macromolecules* **1987**, *20*, 1376.
- ¹⁸ Frenkel, D.; Smit, B. *Understanding Molecular Simulation. From Algorithms to Applications*; Academic Press:New York, 2nd edition, 2002.
- ¹⁹ Allen, M. P.; Tildesley, D. J. *Computer Simulations of Liquids*; Oxford University Press:Oxford, 1987.
- ²⁰ Galperin, D. E.; Ivanov, V. A.; Mazo, M. A. Mazo; Khokhlov, A. R. *Polym. Sci. Ser. A* **2005**, *47*, 61.
- ²¹ Gurtovenko, A. A.; Lyulin, A. V.; Karttunen, M.; Vattulainen, I.; *J. Chem. Phys.* **2006**, *124*, 094904.
- ²² Majtyka, M.; Klos, J. *Phys. Chem. Chem. Phys.* **2007**, *9*, 2284.
- ²³ Korn, G. A.; Korn, T. M. *Mathematical Handbook for Scientists and Engineers*; McGraw-Hill Book Company:New York, 2nd edition, 1968, Appendix B.
- ²⁴ Meier-Kroll, A. A.; Fleck, C. C.; von Grünberg, H. H. *J. Phys.: Condens. Matter* **2004**, *16*, 6041.
- ²⁵ Rädler, J. O.; Koltover, J.; Salditt, T.; Safinya, C. *Science* **1997**, *275*, 810.
- ²⁶ Verma, I. M.; Somia, N. *Nature* **1997**, *389*, 239.
- ²⁷ Evans, H. M.; Ahmad, A.; Ewert, K.; Martin-Herranz, A.; Bruinsma, R. F.; Safinya, C. R. *Phys. Rev. Lett.* **2003**, *91*, 075501.
- ²⁸ Wittemann, A.; Haupt, B.; Ballauff, M. *Phys. Chem. Chem. Phys.* **2003**, *5*, 1671.
- ²⁹ Konieczny, M.; Likos, C. N. *Soft Matter*, **2007**, *3*, 1130.